

Dispersive surface waves along partially saturated porous media

Gabriel Chao^{a)}

Department of Geotechnology, Delft University of Technology, and Department of Applied Physics, Eindhoven University of Technology, P. O. Box 513, 5600 MB Eindhoven, The Netherlands

D. M. J. Smeulders

Department of Geotechnology, Delft University of Technology, P. O. Box 5028, 2600 6A Delft, The Netherlands

M. E. H. van Dongen

Department of Applied Physics, Eindhoven University of Technology, P. O. Box 513, 5600 MB Eindhoven, The Netherlands

(Received 7 July 2005; revised 2 December 2005; accepted 13 December 2005)

Numerical results for the velocity and attenuation of surface wave modes in fully permeable liquid/partially saturated porous solid plane interfaces are reported in a broadband of frequencies (100 Hz–1 MHz). A modified Biot theory of poromechanics is implemented which takes into account the interaction between the gas bubbles and both the liquid and the solid phases of the porous material through acoustic radiation and viscous and thermal dissipation. This model was previously verified by shock wave experiments. In the present paper this formulation is extended to account for grain compressibility. The dependence of the frequency-dependent velocities and attenuation coefficients of the surface modes on the gas saturation is studied. The results show a significant dependence of the velocities and attenuation of the pseudo-Stoneley wave and the pseudo-Rayleigh wave on the liquid saturation in the pores. Maximum values in the attenuation coefficient of the pseudo-Stoneley wave are obtained in the 10–20 kHz range of frequencies. The attenuation value and the characteristic frequency of this maximum depend on the liquid saturation. In the high-frequency limit, a transition is found between the pseudo-Stoneley wave and a true Stoneley mode. This transition occurs at a typical saturation below which the slow compressional wave propagates faster than the pseudo-Stoneley wave. © 2006 Acoustical Society of America.

[DOI: 10.1121/1.2164997]

PACS number(s): 43.20.Jr, 43.20.Gp [RR]

Pages: 1347–1355

I. INTRODUCTION

The presence of gas bubbles can dramatically influence the acoustic properties of a liquid. The bulk modulus of the liquid becomes frequency-dependent and attenuation effects arise due to oscillations of the bubbles (radiation) and heat transfer to the surrounding liquid.¹ It is particularly interesting to consider the problem of a gas-liquid mixture filling the pore space of a porous medium. In this case, even more dissipative mechanisms have to be taken into account, namely the interaction between the gas and both the liquid and the solid elastic matrix. In the case that only liquid saturates the pore space, the interaction between the liquid and the solid matrix can be understood in terms of the Biot theory.^{2,3} This theory was previously extended in order to include the effects of gas saturation on the bulk elastic waves in partially saturated porous media by among others White,⁴ Dutta and Ode,^{5,6} Berryman *et al.*,⁷ Smeulders and Van Dongen,⁸ Johnson,⁹ and Carcione *et al.*¹⁰

A great deal of attention has been given to the influence of the gas saturation on the velocities and attenuation of

seismic waves since the pioneering work of White.⁴ The White model describes the air fraction as spherical gas pockets distributed in a cubic array in the liquid-saturated porous medium. This model will be referred to as the “gas pocket model.” Dutta and Ode^{5,6} provided a more complete solution based on Biot’s theory for the bulk modulus of a single bubble surrounded by a fluid-saturated porous spherical shell. Berryman *et al.*⁷ formulated a model based on variational principles for the bulk acoustic properties of a porous medium saturated with a mixture of two fluids. Experiments were carried out by Smeulders and Van Dongen⁸ on compressional wave propagation in porous columns saturated by an air-water mixture. Their theoretical model is based on the study of the response of a gas bubble in a fully saturated porous medium to an external oscillating pressure field. Damping mechanisms due to radiation into the two compressional waves, viscous dilatation at the bubble surface, and heat exchange with the solid matrix are considered. De-grande *et al.*¹¹ used this model to study the effects of saturation on the wave propagation phenomena in a porous layer adjacent to a water table. An interpretation of laboratory velocity measurements in a variety of partially gas-saturated rocks is given by Gist.¹² Cadoret *et al.*^{13,14} reported experimental results using a resonant-bar technique to determine

^{a)}Electronic mail: g.e.chao@tue.nl

the velocity and attenuation of acoustic waves in partially saturated limestones at a sonic frequency of 1 kHz. Similar experiments were previously performed by Lucet.¹⁵

Despite all the efforts and attention to study saturation effects on seismic and acoustic waves, there is, to our best knowledge, no study concerning the influence of the liquid saturation on surface waves. The purpose of this work is to investigate the effects of the gas fraction on the propagation of surface waves along a plane interface between a liquid and a partially saturated porous medium. The bulk acoustic properties of the partially saturated porous medium are described according to the model of Smeulders and Van Dongen.⁸ The high-frequency properties of the surface waves for the fully saturated case were studied in detail by Feng and Johnson.^{16,17} There are three surface modes that can propagate depending on the relation between the mechanical properties of the porous material and the liquid, and the characteristics of the interface regarding the possibility for the liquid to flow between the two half-spaces (surface permeability). The three modes are the Stoneley wave, the pseudo-Stoneley wave and the pseudo-Rayleigh wave. The Stoneley wave is a true surface wave which propagates almost undamped along the interface with an exponential decay in the normal direction away from the interface. The pseudomodes are significantly damped in the direction of propagation and radiate energy into the slow compressional wave only (pseudo-Stoneley wave) or both into the slow compressional wave and the acoustic wave in the liquid half-space (pseudo-Rayleigh wave). Recently, Gubaidullin *et al.*¹⁸ considered the effects of viscous losses in the dispersive properties of the surface waves. In this paper we consider the influence of gas bubbles in the porous solid on the properties of the surface waves. First we investigate the high-frequency limit, where the viscous interaction can be neglected. Then the frequency-dependent dispersion of the pseudo modes is analyzed.

The paper is organized as follows. In Sec. II we review the theoretical model for acoustic wave propagation for the case that a liquid-gas mixture saturates the porous material. In Sec. III the results for the velocity and attenuation of the surface modes propagating along a liquid-poroelastic plane interface are presented and discussed. First the high-frequency limit is examined and the different waves are discussed, followed by the analysis of the frequency-dependent results. The study is summarized and the conclusions are given in Sec. IV.

II. ACOUSTIC PROPERTIES OF A PARTIALLY SATURATED POROUS MEDIUM

Acoustic wave propagation through a fully saturated porous media can be described in terms of the Biot equations. In the frequency domain these equations are expressed as

$$-\omega^2(\tilde{\rho}_{11}\tilde{\mathbf{u}} + \tilde{\rho}_{12}\tilde{\mathbf{U}}) = (P - N) \nabla \nabla \cdot \tilde{\mathbf{u}} + N \nabla^2 \tilde{\mathbf{u}} + Q \nabla \nabla \cdot \tilde{\mathbf{U}} \quad (1)$$

and

$$-\omega^2(\tilde{\rho}_{12}\tilde{\mathbf{u}} + \tilde{\rho}_{22}\tilde{\mathbf{U}}) = R \nabla \nabla \cdot \mathbf{U} + Q \nabla \nabla \cdot \tilde{\mathbf{u}}, \quad (2)$$

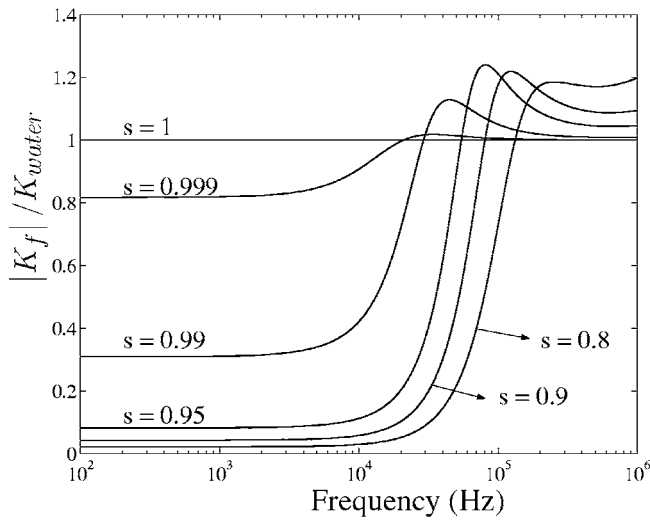
where $\tilde{\mathbf{u}}$ is the solid displacement and $\tilde{\mathbf{U}}$ is the fluid displacement. N is the shear modulus of the composite material and P , Q , and R are the so-called generalized elastic coefficients. They are related to the porosity ϕ , the solid frame bulk modulus K_b , the solid grain bulk modulus K_s , the pore-fluid modulus, K_f and N through the so-called Gedanken experiments. The parameters $\tilde{\rho}_{11}$, $\tilde{\rho}_{12}$, and $\tilde{\rho}_{22}$ are the complex-valued frequency-dependent densities. They are functions of the density of the fluid ρ_f , the density of the solid ρ_s , the porosity ϕ , and the frequency-dependent tortuosity $\tilde{\alpha}(\omega)$. It is not the purpose of this section to review Biot's theory and for further details the reader is referred to classical books on the subject (see, e.g., Allard¹⁹ and Bourbie *et al.*²⁰).

In our case, the pore space is saturated by a mixture of water and air. Therefore, new interaction mechanisms between the gas and the liquid and the gas and the solid matrix have to be taken into account. The oscillations of the air bubbles will induce radiation of the two compressional waves at the bubble surfaces. The liquid dilatation at the bubble surface causes viscous attenuation. Finally, heat transport from the bubble to the surrounding media is also considered. In this work, the dissipative phenomena mentioned above are described in terms of a complex-valued frequency-dependent bulk modulus of the mixture of water and air.⁸ In this section we will review the main results of this theory and analyze its implications for the bulk modes. The compressibility of the solid grains is also considered, which was neglected in the cited paper.⁸ The model is based on the calculation of the volume variation of a single bubble as a response to an external oscillating pressure field (Appendix A). The dynamics of the bubble is determined by the solution of the Biot equations at the spherical interface between the gas-saturated and the liquid-saturated porous media. Mathematically, it is possible to solve the Biot equations in spherical coordinates in the two domains, inside and outside the bubble. The solutions are then matched using appropriate boundary conditions and the bubble volume change due to the harmonic pressure can be calculated. In this way the bulk modulus of the bubble can be computed and, neglecting the interaction between the bubbles it will be considered as the bulk modulus of the gas phase in the mixture, $K_g(\omega)$. The frequency-dependent bulk modulus of the mixture, $K_f(\omega)$ is obtained through a modified Wood's formula²¹

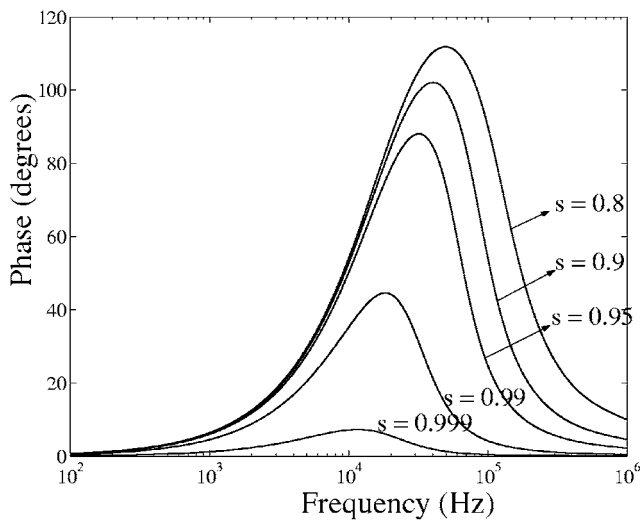
$$\frac{1}{K_f(\omega)} = \frac{s}{K_l} + \frac{1-s}{K_g(\omega)}, \quad (3)$$

where K_l is the bulk modulus of the liquid phase and s is the liquid saturation. The expression for $K_f(\omega)$ given in Eq. (3) differs from the original Wood's formula in which both the bulk modulus for the gas and liquid phases are constant.

Strictly speaking, the original Wood's formula is only valid for highly homogeneous mixtures and at frequencies sufficiently low so that the wavelengths are considerably larger than the size of the heterogeneities. In this case it is possible to assume that the external oscillating pressure field is spatially homogeneous at a local scale. In our case this scale is determined by the size of the gas bubbles and the



(a)



(b)

FIG. 1. Frequency-dependent bulk modulus for a mixture of water and air saturating a Berea sandstone porous rock. The radius of the air bubbles is 1 mm and the gas pressure is 0.01 GPa (100 bars). Different liquid saturation s are considered.

distance between them. This assumption is valid for the range of bubble sizes and frequencies considered in this work. At higher frequencies or heterogeneous mixtures, scattering effects cannot be neglected and it is no longer possible to define a homogeneous external driving pressure at a local scale. In this work a bubble radius of 1 mm is considered, in accordance with experimental values reported for air-water mixtures saturating the pores of artificial sandstones.⁸ In this scenario, a threshold frequency of 1.5 MHz can be defined, below which the assumption of this model is valid. At this threshold frequency, the wavelength of the fast compressional wave equals the diameter of the gas bubble.

Figure 1 shows the absolute and phase values of the bulk modulus of the mixture as a function of the frequency for different liquid saturations. A Berea sandstone saturated by a water-air mixture is considered. The properties of the porous material and the saturating fluids are given in Table I. On one hand, at low frequencies, the bulk modulus of the gas phase equals 0.01 GPa and therefore a decrease in liquid saturation

TABLE I. Physical properties of the Berea sandstone and the saturating fluids: water and air.

Solid density ρ_s (kg/m ³)	2644
Porosity ϕ	0.20
Permeability k_0 (mD)	360
Tortuosity α_∞	2.4
Frame bulk modulus K_b (GPa)	10.37
Shear modulus N (GPa)	7.02
Grain bulk modulus K_s (GPa)	36.5
Liquid bulk modulus K_l (GPa)	2.25
Gas pressure (bulk modulus) p_g (GPa)	0.01
Liquid density ρ_l (kg/m ³)	1000
Gas density ρ_g (kg/m ³)	100
Liquid viscosity η_l (mPa s)	1
Gas viscosity η_g (mPa s)	1.5×10^{-2}
Gas thermal diffusivity a_g	1.8×10^{-7}

causes a decrease in the bulk modulus of the mixture since $K_l > K_g$. On the other hand, at high frequencies, the gas phase becomes highly incompressible ($|K_g| \rightarrow \infty$) and $K_f = K_l/s$. In this limit, K_f increases with concentration of air in the water. The transition between the two limits shows a minimum in the compressibility of the mixture, which corresponds to the antiresonance frequency of the bubble. At this frequency the bubbles oscillate out-of-phase with the external pressure field, which results in a highly incompressible medium. The relevant parameters in this model are the pressure of the gas, its saturation in the pore space, and the radius of the gas bubbles. The outcome of the velocities and attenuation of the compressional waves that propagate in this partially saturated porous media are shown in Fig. 2 for a liquid saturation s of 0.95 and a bubble radius of 1 mm. The results for the wave velocities can be explained by the arguments about the changes in the compressibility of the mixture discussed above. The presence of air decreases the bulk modulus of the mixture at low frequencies which results in compressional waves propagating slower in the partially saturated case. This behavior is reversed at high frequencies where the compressional waves propagate faster when the air saturation is increased. More interesting are the modifications induced by the air phase in the attenuation coefficients. The decrease in the liquid content of the mixture result in a significant increase of the attenuation for the fast compressional wave, which is observed throughout the complete range of frequencies studied. The slow compressional wave presents a maximum in the attenuation for the partially saturated case. This maximum is not observed for the fully saturated case. The model presented here assumes that the shear wave is influenced by the presence of the gas phase only due to changes in density. The frequency-dependent mechanisms incorporated in this model have been experimentally corroborated by shock-induced transmission/reflection wave experiments carried out in a shock tube.⁸

III. SATURATION EFFECTS ON THE VELOCITIES AND ATTENUATION OF THE SURFACE WAVES

In this section the numerical results for the phase velocities and attenuation coefficients of the surface wave modes

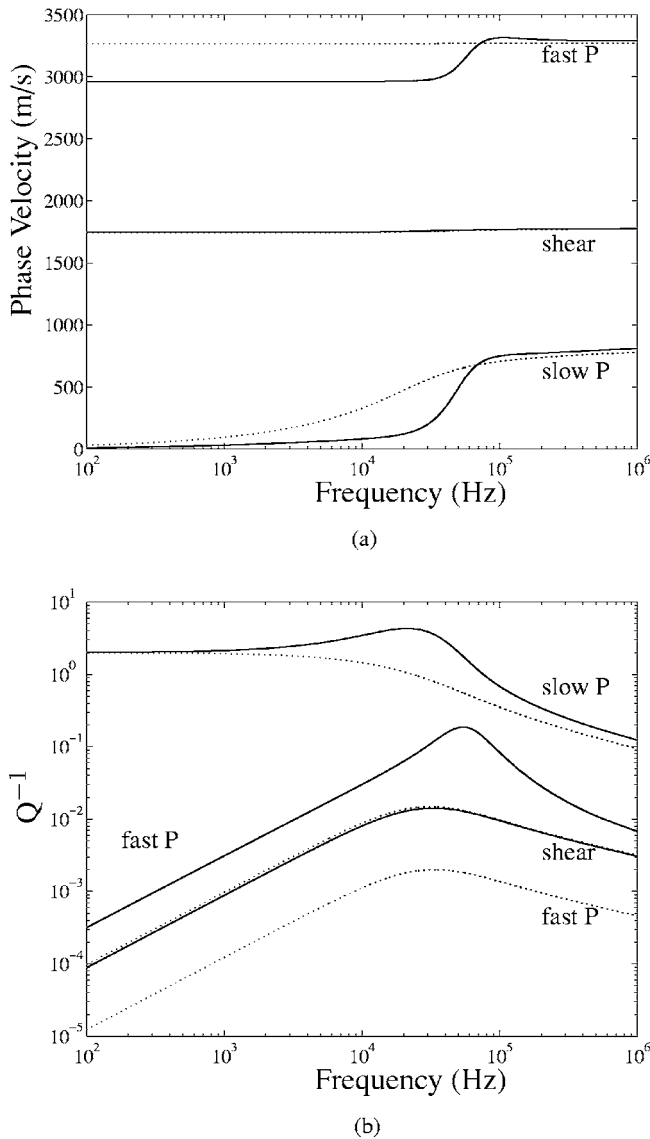


FIG. 2. Phase velocities (a) and attenuation coefficients (b) of the body waves in a water/air-saturated Berea sandstone. The effects of air saturation are shown for the compressional waves in solid lines, the gas pressure is 0.01 GPa, the bubble radius 1 mm, and $s=0.95$. The Biot predictions for the fully saturated case are shown in dotted lines.

that propagate along a liquid/partially saturated poroelastic plane interface are discussed. The configuration is depicted in Fig. 3. The mathematical procedure involves the numerical solution of the boundary value problem which follows

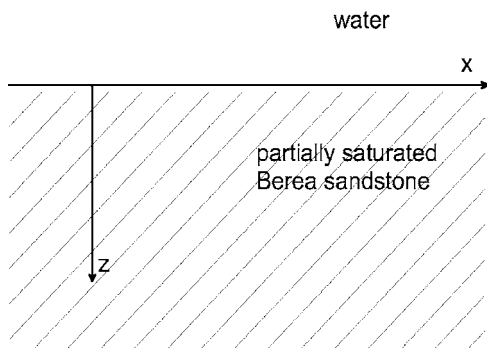
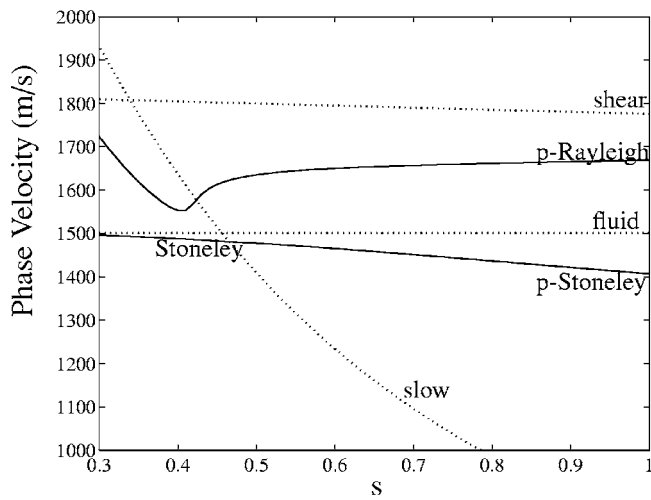


FIG. 3. Liquid/partially saturated porous medium plane interface.

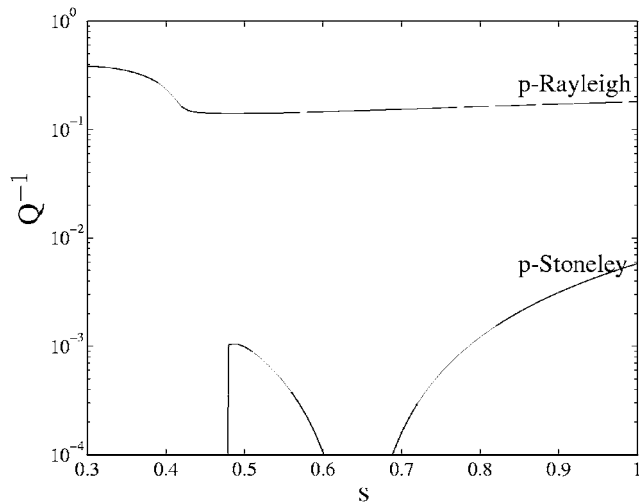
from the application of the boundary conditions at the interface (see Appendix B). The oscillating gas bubble model⁸ outlined in the previous section is employed to describe the bulk modulus of the fluid phase, which in this case is composed of a mixture of water and air. The properties of the solid matrix correspond to the Berea sandstone characterized in Table I. We adopt the surface wave terminology given by Feng and Johnson.¹⁶ In order to avoid confusion, it is worthwhile to mention that the pseudo-Stoneley wave propagating along a liquid/poroelastic interface is the generalization of the classical Stoneley wave in a liquid/elastic interface. In the poroelastic case it becomes a pseudo wave due to radiation into the slow P wave. It is important to note that in this work we will assume that the interface is fully permeable so that continuity of pressure holds across the interface. The effect of sealed or partially sealed pores at the interface has been modelled in the past using the empirical concept of surface flow impedance. We restrict ourselves to the open pore boundary case.

We first examine the high-frequency limit, for which the velocities of the bulk modes become real valued and the slow wave is propagative. It also holds that the bulk modulus of the mixture saturating the pore space becomes real-valued (K_f/s). Therefore, the dissipative mechanisms induced by the oscillation of the gas bubbles are not present in this limit as can be clearly observed in Fig. 1. The dependence of the surface wave velocities and attenuation on the water saturation is shown in Fig. 4. For reference, the bulk wave velocities are also displayed.

For the fully water-saturated case $s=1$, two surface modes are found: the pseudo-Stoneley wave and the pseudo-Rayleigh wave. The pseudo-Stoneley wave has a velocity which is faster than the velocity of the slow wave and slower than the speed of the rest of the bulk modes. This implies that it radiates energy into the slow wave and therefore it is called a pseudo or leaky mode. The pseudo-Rayleigh wave leaks energy into the fluid half-space and into the slow wave, its velocity is faster than that of the slow wave and the fluid wave but slower than that of the shear and the fast wave (the fast wave is not plotted). The velocity of the slow wave decreases with increasing water saturation as can be observed in Fig. 4, while the shear mode speed is slightly affected due to density effects only. The behavior of the slow wave as a function of saturation and its relation with the other bulk modes plays an important role in the properties of the surface waves. For water saturations higher than 0.47, the velocity of the pseudo-Stoneley wave is higher than that of the slow wave. In this range of saturations both the pseudo-Stoneley wave and the pseudo-Rayleigh wave exist. The velocity of the pseudo-Stoneley wave decreases with increasing water saturation. For s values below 0.47 the pseudo-Stoneley wave becomes a true Stoneley wave due to the fact that the slow wave becomes faster than it. This transition is neatly illustrated in the attenuation coefficient [Fig. 4(b)], which shows the attenuation in terms of the inverse quality factor Q^{-1} . When the pseudo-Stoneley wave becomes the true Stoneley wave, the damping necessarily disappears because radiation ceases to exist for saturation values below 0.47. The attenuation of the pseudo-Stoneley wave has a



(a)

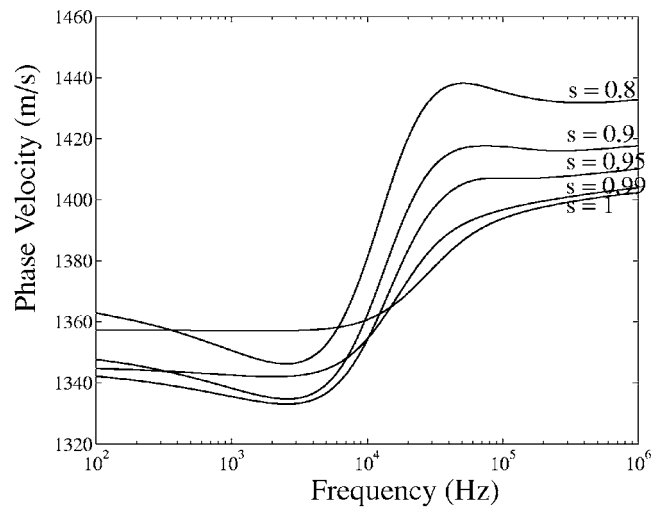


(b)

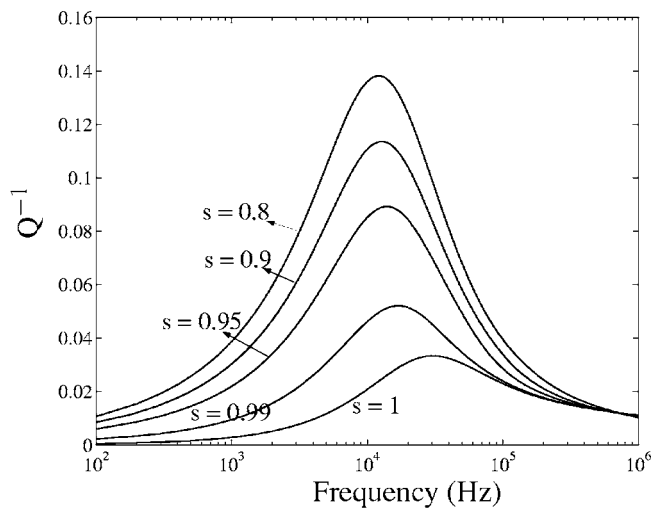
FIG. 4. Saturation effects on the phase velocity (a) and attenuation (b) of the surface waves that propagate in a flat interface between water and a porous Berea sandstone saturated by a mixture of air and water. The high-frequency limit is considered. The bulk wave velocities are plotted in dashed lines.

sharp minimum at 0.64 and over the entire range of saturations it is significantly less damped than the pseudo-Rayleigh mode. The pseudo-Rayleigh wave ceases to radiate into the slow wave for water saturations below 0.43, because its velocity becomes lower than that of the slow wave. A sharp increase in Q^{-1} is observed for water saturations below 0.43 where the pseudo-Rayleigh wave ceases to radiate into the slow wave. The only dissipative mechanism here is radiation into the fluid wave. It is worthwhile to note that the study of the high-frequency limit provides a first insight on the compressibility effects on the surface modes due to the presence of the gas fraction.

We now extend the study to more realistic frequency-dependent surface waves and we consider the dissipative mechanisms which were neglected previously. In this case we calculate the dispersive results for the leaky modes for different liquid saturations. Figure 5 shows the results for the pseudo-Stoneley wave. The phase velocity decreases with



(a)

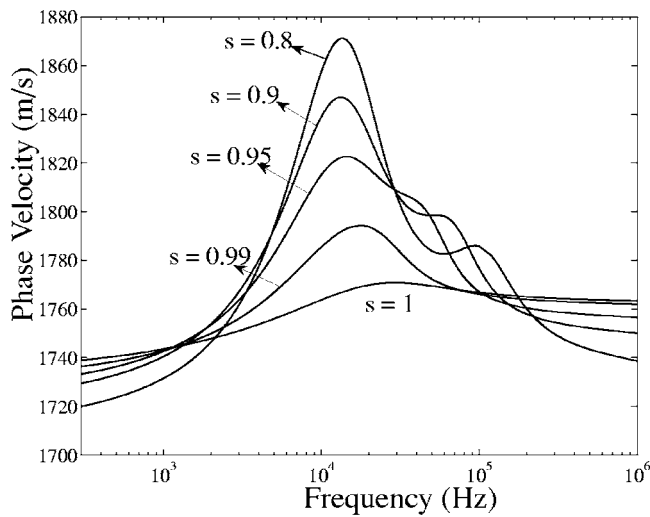


(b)

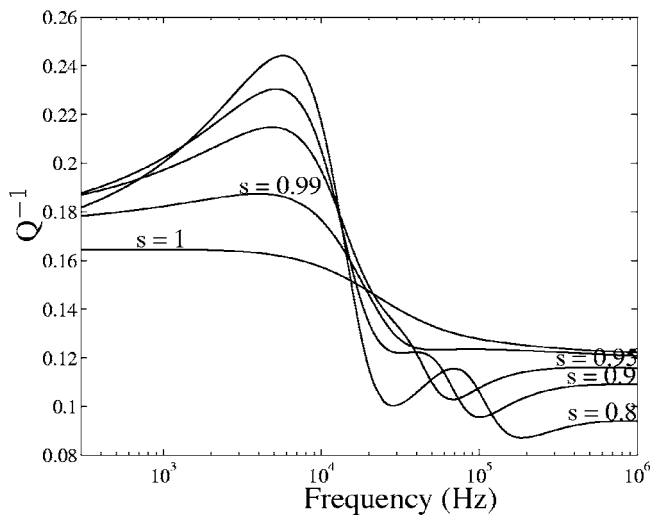
FIG. 5. Frequency-dependent phase velocities (a) and attenuation coefficients (b) of the pseudo-Stoneley wave along a water/partially saturated poroelastic interface. The porous material is a Berea sandstone saturated with a water-air mixture. Different liquid saturations s are considered.

saturation at high frequencies. This is consistent with the high-frequency results. At low frequencies, the phase velocities are considerably less than at high frequencies for all saturations, although a clear trend with saturation is not found. The results for the attenuation coefficient show a monotonous increase with the air fraction occupying the pore space. This influence of the gas fraction is most significant in the 1–100 kHz range. The characteristic frequency for the maximum of Q^{-1} depends on saturation. It is found that when s increases this characteristic frequency moves towards higher values.

The influence of the saturation on the properties of the pseudo-Rayleigh is depicted in Fig. 6. At low and high frequencies the pseudo-Rayleigh wave propagates slower when the liquid fraction in the pore space is decreased. Interesting features occur at intermediate frequencies (1–150 kHz). In this range of frequencies the speed of the pseudo-Rayleigh mode decreases with increasing saturation. Furthermore, a



(a)



(b)

FIG. 6. Frequency-dependent phase velocities (a) and attenuation coefficients (b) of the pseudo-Rayleigh wave in a water/partially saturated poroelastic interface. The porous material is a Berea sandstone saturated with a water-air mixture. Different liquid saturations s are considered.

peak in the phase velocity is predicted. For the values of liquid saturation studied in this work, this maximum lies in frequencies between 10 and 20 kHz. The position of this maximum on the frequency axis slightly depends on saturation; lower characteristic frequencies are obtained for lower values of s . It is interesting to note the presence of additional local maxima for the $s=0.95$, $s=0.9$, and $s=0.8$ cases, which become more pronounced for lower saturation values. The characteristic frequency of this secondary maximum increases with decreasing saturation.

The higher attenuation values are obtained in the low-frequency range and a maximum is observed. This maximum is associated with the presence of air bubbles and becomes sharper when the saturation decreases. For the lower liquid saturation cases considered here, $s=0.9$ and $s=0.8$, a second local maximum is observed at higher frequencies. The at-

tenuation coefficient Q^{-1} diminishes at high frequencies and in this limit a clear dependence on liquid saturation is found where the attenuation increases with saturation.

IV. CONCLUSIONS AND DISCUSSION

In this work we have studied the saturation effects on the properties of the surface waves that propagate along a plane interface between a liquid and a partially saturated porous solid. The numerical results for the pseudo-Stoneley wave and the pseudo-Rayleigh wave show interesting features when the pore space of the poroelastic medium is filled with a mixture of water and air. In the high-frequency limit where only compressibility effects are present, the full range of liquid saturations was studied. A transition between the leaky pseudo-Stoneley wave and the true Stoneley wave is found at a characteristic saturation for which the slow P wave propagates faster than the pseudo-Stoneley wave. This transition is neatly illustrated in the behavior of the attenuation coefficient Q^{-1} which drastically decreases for water saturations lower than $s=0.46$. This indicates that the pseudo-Stoneley wave becomes a true unattenuated surface wave, the Stoneley wave.

When the frequency-dependent dissipative mechanisms are included, interesting features arise in the velocity and attenuation of the surface waves. The pseudo-Stoneley wave shows a well-defined maximum in the attenuation. This maximum is located in the range of frequencies which is relevant to borehole geophysical applications (5–30 kHz). The characteristic frequency of this maximum depends on the liquid saturation. In acoustic borehole logging techniques the pseudo-Stoneley plays an important role in reservoir characterization. In this context, our numerical results indicate that the attenuation of the pseudo-Stoneley can provide valuable information on the liquid saturation in the pores. Similar conclusions can be drawn for the phase velocity of the pseudo-Rayleigh wave though it should be noted that this wave is difficult to detect in field or laboratory measurements. An independent determination of the bubble size remains the main obstacle for a direct application of this model to practical situations.

ACKNOWLEDGMENT

This study was supported by the ISES (Integrated Solid Earth Sciences) program.

APPENDIX A: FREQUENCY-DEPENDENT BULK MODULUS $K_g(\omega)$

The purpose of this appendix is to highlight the main conceptual steps involved in the derivation of the complex-valued bulk modulus of the gas phase, $K_g(\omega)$. In the remaining of the appendixes and in order to simplify the notation, the tilde above the functions and quantities in the frequency domain is omitted. The tilde above the density terms and the tortuosity is used to denote the frequency-dependent nature of these functions (see, e.g., Allard¹⁹).

Let us consider a spherical air bubble immersed in a fully water saturated porous medium in the presence of an external oscillating pressure field. First, we will focus on the

external domain (fully water-saturated porous medium outside the bubble). We introduce the displacement potentials Φ_{c1} and Φ_{c2} associated with the fast wave and the slow compressional wave as follows:

$$\mathbf{u} = \nabla\Phi_{c1} + \nabla\Phi_{c2}, \quad (\text{A1})$$

and

$$\mathbf{U} = G_{c1} \nabla\Phi_{c1} + G_{c2} \nabla\Phi_{c2}, \quad (\text{A2})$$

where

$$G_{c1} = \frac{P - v_{c1}^2 \tilde{\rho}_{11}}{v_{c1}^2 \tilde{\rho}_{12} - Q}, \quad (\text{A3})$$

and

$$G_{c2} = \frac{P - v_{c2}^2 \tilde{\rho}_{11}}{v_{c2}^2 \tilde{\rho}_{12} - Q}. \quad (\text{A4})$$

In the above equations v_{c1} and v_{c2} refer to the frequency-dependent wave velocities of the fast wave and the slow wave.

Assuming an $e^{i\omega t}$ temporal variation, the linearized radial momentum equation for the liquid phase can be written as follows:

$$\omega^2 \phi \rho_f U_r = \phi \frac{\partial p_f}{\partial r} + [\tilde{\alpha}(\omega) - 1] \omega^2 \phi \rho_f (u_r - U_r). \quad (\text{A5})$$

The above equation is integrated from the bubble radius ($r = a$) to infinity in order to find an equation of motion for the bubble, which reads

$$\begin{aligned} \phi \rho_f \omega^2 (G_{c1} \Phi_{c1} + G_{c2} \Phi_{c2}) = & -\phi (p_{f\infty} - p_{fa}) \\ & + \omega^2 \phi \rho_f [\tilde{\alpha}(\omega) - 1] [\Phi_{c1a} (1 \\ & - G_{c1}) + \Phi_{c2a} (1 - G_{c2})]. \end{aligned} \quad (\text{A6})$$

We seek solutions for the potentials outside the bubble in the form

$$\Phi_{c1} = \frac{A_{c1} e^{-ik_1 r}}{r}, \quad (\text{A7})$$

and

$$\Phi_{c2} = \frac{A_{c2} e^{-ik_2 r}}{r}, \quad (\text{A8})$$

where k_1 and k_2 are the radial wave numbers associated with the fast compressional wave and the slow compressional wave respectively. Then, substitution of the solutions given by Eqs. (A7) and (A8) into Eq. (A6), leads to the momentum equation in terms of the two unknowns A_{c1} and A_{c2} . The boundary conditions at the bubble surface provide the remaining relations to close the problem. Inside the bubble we neglect the interaction between the air and the solid matrix and the matrix is considered as acoustically compact. It can be shown that this condition implies that the velocity of the solid phase linearly depends on r . We assume continuity of the radial velocity of the solid phase and its radial derivative across the bubble surface. This last condition allows a closed

analytical solution and it is consistent with numerical calculations based on the gas pocket model.^{5,6} This leads to the following relation:

$$\frac{\partial^2 u_r}{\partial r \partial t}(a^+) = \frac{1}{r} \frac{\partial u_r}{\partial t}(a^+), \quad (\text{A9})$$

which holds at the outside of the bubble (a^+). The continuity of fluid volume provides an equation for the change in the volume of the gas bubble ΔV_g in terms of the fluid and solid displacements at the bubble surface

$$\Delta V_g = 4\pi a^2 [(1 - \phi)u_r + \phi U_r]. \quad (\text{A10})$$

We also consider that the pressure difference across the bubble surface is balanced by the radial viscous stress in the fluid at the bubble surface

$$p_f(a^+) - p_g = \frac{4}{3} \eta \frac{\partial^2 U_r}{\partial r \partial t}(a), \quad (\text{A11})$$

where $p_f(a^+)$ denotes the pressure outside the bubble evaluated at the bubble radius and p_g is the gas pressure inside the bubble.

Substitution of the expressions for Φ_{c1} and Φ_{c2} in the boundary conditions [Eqs. (A9)–(A11)], followed by some algebraic manipulations lead to the following relation between the volume of the air bubble and the external pressure $p_{f\infty}$:

$$\begin{aligned} \omega^2 \rho_f \left[\frac{a_1 b_2 - a_2 b_1}{a_1 c_2 - a_2 c_1} + \frac{4 i \eta \phi a_1 a_2 (G_{c2} - G_{c1})}{3 \omega \rho_f (a_1 c_2 - a_2 c_1)} \right] \frac{V_g}{4\pi \phi a} \\ = p_{f\infty} - p_g, \end{aligned} \quad (\text{A12})$$

where

$$a_j = k_j^2 \left(1 - 3 \frac{1 + ik_j a}{k_j^2 a^2} \right), \quad (\text{A13})$$

$$b_j = \phi G_{c_j} - (G_{c_j} - 1) \frac{\tilde{\rho}_{12} + \phi \rho_f \tilde{\alpha}(\omega)}{\rho_f}, \quad (\text{A14})$$

and

$$c_j = (1 + ik_j a)(1 - \phi + \phi G_{c_j}). \quad (\text{A15})$$

The last dissipative mechanism considered in this model is the thermal damping. It arises due to the heat exchange between the gas phase and the solid matrix induced by the oscillations of the bubble. Its contribution to the bulk modulus of the gas phase can be expressed as $n p_g$. Here we have introduced a complex-valued polytropic coefficient, n :

$$\begin{aligned} n = \gamma \left(1 + 3(\gamma - 1) \left\{ \frac{\coth[\psi(8\alpha_{zg}k_0/\phi)^{1/2}]}{\psi(8\alpha_{zg}k_0/\phi)^{1/2}} \right. \right. \\ \left. \left. - \frac{1}{[\psi(8\alpha_{zg}k_0/\phi)^{1/2}]^2} \right\} \right)^{-1}, \end{aligned} \quad (\text{A16})$$

where $\psi = (1 + i)(\omega/2a_g)$, a_g being the thermal diffusivity of the gas and γ being the specific heat ratio of the gas (for air $\gamma = 1.4$). Champoux and Allard²² and Henry *et al.*²³ reported a slightly different expression for the polytropic exponent n .

Finally, the following expression is found for the frequency-dependent bulk modulus of the gas phase $K_g = -V_g(\partial V_g / \partial p_{fg})^{-1}$:

$$K_g(\omega) = \frac{1}{3} a^2 \omega^2 \rho_f \left[\frac{3n p_g}{a^2 \omega^2 \rho_f} - \frac{a_1 b_2 - a_2 b_1}{a_1 c_2 - a_2 c_1} - \frac{4 i \eta \phi a_1 a_2 (G_{c2} - G_{c1})}{3 \omega \rho_f (a_1 c_2 - a_2 c_1)} \right]. \quad (A17)$$

APPENDIX B: DISPLACEMENT POTENTIAL FORMULATION FOR THE SURFACE MODES

In this appendix a displacement potential formulation is developed in order to describe the surface waves that propagate along a plane interface between a fluid half-space and a liquid-saturated porous half-space. The configuration studied is displayed in Fig. 3.

The surface modes propagate parallel to the interface, depend exponentially on the distance z from the interface and can be expressed in terms of the bulk mode solutions. In the liquid ($z < 0$), the compressional waves are described by the following potential:

$$\Phi_f = A_f e^{\gamma_f z} e^{i(k_x x - \omega t)}. \quad (B1)$$

The potentials associated to each of the bulk modes which propagate in the porous half-space are

$$\Phi_{c1} = A_{c1} e^{-\gamma_{c1} z} e^{i(k_x x - \omega t)}, \quad (B2)$$

$$\Phi_{c2} = A_{c2} e^{-\gamma_{c2} z} e^{i(k_x x - \omega t)}, \quad (B3)$$

and

$$\Psi_{sh} = B e^{-\gamma_{sh} z} e^{i(k_x x - \omega t)} \hat{e}_y, \quad (B4)$$

where \hat{e}_y is the cartesian basis vector in the y direction. The above potentials describe waves that propagate parallel to the interface. The wave numbers in the z direction are related to the horizontal wave number k_x through the following relations:

$$\gamma_j = \sqrt{k_x^2 - \frac{\omega^2}{c_j^2}}, \quad j = 1, 2, sh, f, \quad (B5)$$

where c_j is the velocity of the corresponding bulk mode.

The surface modes can be written as a frequency-dependent linear combination of the potentials stated above. The different contributions of the bulk modes are determined by the boundary conditions, namely: continuity of averaged normal displacement, total stress, and pressure. The displacements of the solid phase and the fluid phase in the porous medium can be expressed as follows:

$$\mathbf{u} = \nabla(\Phi_{c1} + \Phi_{c2}) + \nabla \times \Psi_{sh}, \quad (B6)$$

and

$$\mathbf{U} = G_{c1} \nabla \Phi_{c1} + G_{c2} \nabla \Phi_{c2} + G_{sh} \nabla \times \Psi_{sh}, \quad (B7)$$

where \mathbf{u} refers to the displacement of the matrix and \mathbf{U} to the displacement of the pore fluid. In the liquid half-space, the displacement \mathbf{U}_f is $\nabla \Phi_f$. Therefore the continuity of average normal displacement at the interface

$$(1 - \phi)u_z + \phi U_z = U_{fz}, \quad (B8)$$

can be expressed as:

$$(1 - \phi + \phi G_{c1}) \frac{\partial \Phi_{c1}}{\partial z} + (1 - \phi + \phi G_{c2}) \frac{\partial \Phi_{c2}}{\partial z} + (1 - \phi + \phi G_{sh}) \frac{\partial \Psi_{sh}}{\partial x} = \frac{\partial \Phi_f}{\partial z}. \quad (B9)$$

The continuity of the normal component of the total stress implies

$$\tau_{zz} - \phi p = -p_f. \quad (B10)$$

Using the Biot's stress-strain relations (see, e.g., Allard¹⁹), the above equation can be written in terms of the potentials as follows:

$$[P - 2N + Q + G_{c1}(Q + R)] \nabla^2 \Phi_{c1} + 2N \frac{\partial^2 \Phi_{c1}}{\partial z^2} + [P - 2N + Q + G_{c2}(Q + R)] \nabla^2 \Phi_{c2} + 2N \frac{\partial^2 \Phi_{c2}}{\partial z^2} + 2N \frac{\partial^2 \Psi_{sh}}{\partial z \partial x} = -\omega^2 \rho_w \Phi_f. \quad (B11)$$

The absence of tangential stress in the liquid requires $\tau_{xz} = 0$ at the interface, and this condition implies that

$$N \left[2 \left(\frac{\partial^2 \Phi_{c1}}{\partial z \partial x} + \frac{\partial^2 \Phi_{c2}}{\partial z \partial x} \right) + \frac{\partial^2 \Psi_{sh}}{\partial x^2} - \frac{\partial^2 \Psi_{sh}}{\partial z^2} \right] = 0. \quad (B12)$$

Finally, the continuity of pressure leads to

$$-\frac{1}{\phi} [(Q + R G_{c1}) \nabla^2 \Phi_{c1} + (Q + R G_{c2}) \nabla^2 \Phi_{c2}] = \rho_w \omega^2 \Phi_f. \quad (B13)$$

Substituting Eqs. (B1)–(B4) into Eqs. (B9) and (B11)–(B13) and after some algebraic manipulations a linear system for the amplitudes of the potentials is found

$$\mathbf{N}(k_x, \omega) \cdot \mathbf{a} = 0, \quad (B14)$$

where the matrix \mathbf{N} contains information about the mechanical properties of the fully saturated porous medium and the water half-space and \mathbf{a} is a vector containing the amplitude of the wave potentials, $\mathbf{a}^T = (A_f, A_{c1}, A_{c2}, B)$. The elements of the matrix \mathbf{N} are given in Appendix C. The surface modes satisfy the condition that the determinant of \mathbf{N} equals zero

$$\det[\mathbf{N}(k_x, \omega)] = 0. \quad (B15)$$

At a fixed frequency ω , Eq. (B15) is numerically solved for complex k_x using a Newton-Raphson algorithm. In this way, frequency-dependent phase velocities, $V(\omega) = \omega \text{Re}^{-1}(k_x)$, and specific attenuation coefficients, $Q^{-1}(\omega) = 2 |\text{Im}(k_x) / \text{Re}(k_x)|$ are obtained. The frequency-dependent bulk modulus of the mixture of fluids $K_f(\omega)$, enters the model via the generalized elastic coefficients P , Q , and R , which themselves also influence the complex velocities of the compressional waves $c1$ and $c2$.

APPENDIX C: MATRIX COEFFICIENTS

In this appendix the elements n_{ij} of the matrix \mathbf{N} of Eq. (B14) are explicitly given

$$n_{11} = \gamma_f,$$

$$n_{12} = \gamma_{c1}(1 - \phi + \phi G_{c1}),$$

$$n_{13} = \gamma_{c2}(1 - \phi + \phi G_{c2}),$$

$$n_{14} = -ik_x(1 - \phi + \phi G_{sh}),$$

$$n_{21} = 0,$$

$$n_{22} = 2N\gamma_{c1}ik_x,$$

$$n_{23} = 2N\gamma_{c2}ik_x,$$

$$n_{24} = (\gamma_{sh}^2 + k_x^2)N,$$

$$n_{31} = \omega^2 \rho_f,$$

$$n_{32} = -[(P - 2N) + Q + G_{c1}(Q + R)]\left(\frac{\omega}{c_1}\right)^2 + 2N\gamma_{c1}^2,$$

$$n_{33} = -[(P - 2N) + Q + G_{c2}(Q + R)]\left(\frac{\omega}{c_2}\right)^2 + 2N\gamma_{c2}^2,$$

$$n_{34} = -2Nik_x\gamma_{sh},$$

$$n_{41} = \omega^2 \rho_f,$$

$$n_{42} = -\left(\frac{\omega}{c_1}\right)^2 \frac{1}{\phi}(Q + RG_{c1}),$$

$$n_{43} = -\left(\frac{\omega}{c_2}\right)^2 \frac{1}{\phi}(Q + RG_{c2}),$$

$$n_{44} = 0.$$

¹L. Van Wijngaarden, "One dimensional flow of liquids containing small gas bubbles," *Annu. Rev. Fluid Mech.* **4**, 369–395 (1972).

²M. A. Biot, "Theory of propagation of elastic waves in a fluid-saturated porous solid. I: Low-frequency range," *J. Acoust. Soc. Am.* **28**, 168–178 (1956).

³M. A. Biot, "Theory of propagation of elastic waves in a fluid-saturated porous solid. II: Higher frequency range," *J. Acoust. Soc. Am.* **28**, 179–191 (1956).

⁴J. E. White, "Computed seismic speeds and attenuation in rocks with partial gas saturation," *Geophysics* **40**, 224–232 (1975).

⁵N. C. Dutta and H. Ode, "Attenuation and dispersion of compressional waves in fluid-filled porous rocks with partial gas saturation (White model)—Part I: Biot theory," *Geophysics* **44**, 1777–1788 (1979).

⁶N. C. Dutta and H. Ode, "Attenuation and dispersion of compressional waves in fluid-filled porous rocks with partial gas saturation (White model)—Part II: Results," *Geophysics* **44**, 1789–1805 (1979).

⁷J. G. Berryman, L. Thigpen, and R. C. Y. Chin, "Bulk elastic wave propagation in partially saturated porous solids," *J. Acoust. Soc. Am.* **84**, 360–373 (1988).

⁸D. M. J. Smeulders and M. E. H. van Dongen, "Wave propagation in porous media containing a dilute gas-liquid mixture: Theory and experiments," *J. Fluid Mech.* **343**, 351–373 (1997).

⁹D. L. Johnson, "Theory of frequency dependent acoustics in patchy-saturated porous media," *J. Acoust. Soc. Am.* **110**, 682–694 (2001).

¹⁰J. M. Carcione, H. B. Helle, and N. H. Pham, "White's model for wave propagation in partially saturated rocks: Comparison with poroelastic numerical experiments," *Geophysics* **68**, 1389–1398 (2003).

¹¹G. Degrande, G. De Roeck, P. Van Den Broeck, and D. Smeulders, "Wave propagation in layered dry, saturated and unsaturated poroelastic media," *Int. J. Solids Struct.* **35**, 4753–4778 (1998).

¹²G. A. Gist, "Interpreting laboratory velocity measurements in partially gas-saturated rocks," *Geophysics* **59**, 1100–1109 (1994).

¹³T. Cadoret, D. Marion, and B. Zinszner, "Influence of frequency and fluid distribution on elastic wave velocities in partially saturated limestones," *J. Geophys. Res., [Solid Earth]* **100**, 9789–9803 (1995).

¹⁴T. Cadoret, G. Mavko, and B. Zinszner, "Fluid distribution effect on sonic attenuation in partially saturated limestones," *Geophysics* **63**, 154–160 (1998).

¹⁵N. Lucet, P. N. Rasolofosaon, and B. Zinszner, "Sonic properties of rocks under confining pressure using the resonant bar technique," *J. Acoust. Soc. Am.* **89**, 980–990 (1991).

¹⁶S. Feng and D. L. Johnson, "High-frequency acoustic properties of a fluid/porous solid interface. I: New surface mode," *J. Acoust. Soc. Am.* **74**, 906–914 (1983).

¹⁷S. Feng and D. L. Johnson, "High-frequency acoustic properties of a fluid/porous solid interface. II: The 2D reflection green's function," *J. Acoust. Soc. Am.* **74**, 915–914 (1983).

¹⁸A. A. Gubaidullin, O. Yu. Kuchugurina, D. M. J. Smeulders, and C. J. Wisse, "Frequency-dependent acoustic properties of a fluid/porous solid interface," *J. Acoust. Soc. Am.* **116**, 1474–1980 (2004).

¹⁹J. F. Allard, *Propagation of Sound in Porous Media* (Elsevier Science, New York, 1993).

²⁰Th. Bourbié, O. Coussy, and B. Zinszner, *Acoustics of Porous Media* (Gulf, Houston, 1987).

²¹A. B. Wood, *A Textbook of Sound* (Bell, London, 1955).

²²Y. Champoux and J. F. Allard, "Dynamic tortuosity and bulk modulus in air-saturated porous media," *J. Appl. Phys.* **70**, 1795–1797 (1991).

²³M. Henry, P. Lemarinier, J. F. Allard, J. L. Bonardet, and A. Gedeon, "Evaluation of the characteristic dimensions for porous sound-absorbing materials," *J. Appl. Phys.* **77**, 17–20 (1995).